

# Development of an Optical Technology-Based Sensor and Deep Learning Models to Estimate User-Interaction Forces in Smart Walkers

Daniel E. Garcia A.<sup>a, b</sup>, Marcelo Eduardo Vieira Segatto<sup>a, b</sup>, Anselmo Frizera Neto<sup>a, b</sup>, Carlos A. Cifuentes<sup>c</sup>, and Camilo A. R. Diaz<sup>a, b</sup>

<sup>a</sup>Electrical Engineering Department, Universidade Federal do Espiritu Santo. Brazil

<sup>b</sup>Telecommunications Laboratory (LabTel), Universidade Federal do Espiritu Santo. Brazil

<sup>c</sup>Bristol Robotics Laboratory, University of the West of England. United Kingdom

## ABSTRACT

In response to the rising prevalence of mobility-related pathologies and the need to develop technologies capable of constantly monitoring the physical interaction with the user, this study introduces an innovative sensor for robotic walkers. Integrating visible light-sensitive photodiodes and addressable RGB LEDs, the sensor utilizes overlapping signals from embedded emitters and receivers in a transparent flexible waveguide layer to measure tactile deformation. This novel approach overcomes limitations of traditional sensors (i.e. strain gauges, resistive or piezoelectric sensors and, high-resolution triaxial cells) such as fragility and high costs, offering a more accessible alternative. Additionally, deep learning methods demonstrated accurate estimation of the applied normal force with an average error of 2.2%, while the random forest model achieved a classification accuracy of 98% for the contact zones. Designed for seamless integration, the sensor promises to enhance functionality and reduce costs in robotic assistive devices, opening new possibilities in mobility care.

**Keywords:** Robotic Assistive Devices, Smart Walkers, Deep Learning, Force Sensor

## 1. INTRODUCTION

The world is witnessing an unprecedented demographic transformation, with the global population facing a steep rise in aging.<sup>1</sup> According to the World Health Organization, the proportion of individuals over 60 years old is expected to double by 2050, reaching 2.1 billion people.<sup>2</sup> This shift represents significant challenges for healthcare systems, as older adults often experience deterioration in physical functions such as mobility and balance, increasing the risk of falls and injuries that compromise their independence.<sup>3,4</sup> Additionally, chronic noncommunicable diseases, such as cardiovascular and neurological disorders, become more prevalent with age, further limiting dependence in daily life.<sup>5</sup> Therefore, there is a global need to develop innovative solutions and approaches to assist people with reduced mobility.

Robotic walkers have emerged as a promising solution for enhancing mobility, due their simple mechanical design and versatile interaction interfaces.<sup>6,7</sup> These devices integrate advanced modules, including autonomous navigation, biomechanical monitoring, safety systems, obstacle avoidance, and user detection strategies, providing comprehensive physical, cognitive, and sensory support.<sup>8,9</sup> Among these modules, mechanisms for detecting user movement intentions are crucial in facilitating natural and intuitive interactions during gait.<sup>10</sup> These mechanisms enable the walker to interpret the user's physical inputs (typically through sensors located in the handles or base) to dynamically adjust its behavior and ensure a seamless gait experience.<sup>9,10</sup> Traditionally, technologies such as load cells, resistive or piezoelectric sensors, and high-resolution triaxial cells have been employed for this purpose.<sup>3</sup> However, these sensors present significant limitations, including fragility, susceptibility to electromagnetic interference, sensitivity to misalignments, lower compactness, necessity of frequent calibration, and high production costs.<sup>11,12</sup> These drawbacks hinder their integration and effective use in robotic assistive devices, compromising durability and measurement accuracy.

---

Further author information: (Send correspondence to Camilo A. R. Diaz)

E-mail: camilo.diaz@ufes.br

Optical fiber sensors, particularly polymer optical fibers (POF) and fiber Bragg gratings (FBG), represent a promising alternative to conventional force sensors in assistive technologies.<sup>11</sup> POF sensors have been successfully applied to monitor plantar pressure in gait analysis,<sup>13</sup> measure human-robot interaction forces in exoskeletons,<sup>14</sup> and evaluate spring deflection in series elastic actuators,<sup>15</sup> offering advantages such as flexibility, biocompatibility, and resistance to electromagnetic interference. Similarly, FBG sensors provide high-precision measurements in distributed sensing applications, including multipoint force monitoring in robotic devices and structural health monitoring of assistive equipment. However, the high cost of interrogation systems limits their use.<sup>11,16</sup>

Moreover, exist another innovative, cost-effective and scalable alternative based on optical technology. The breakthrough lies in using overlapping signals from light emitters and receivers embedded in a transparent waveguide layer covering the functional areas of the sensor. By measuring the light transport between each emitter and receiver, signals were obtained that varied in response to sensor deformation due to touch, obtaining an estimate of the contact force with high accuracy.<sup>17</sup> Unlike POF and FBG sensors, they present lower hysteresis, are less affected by environmental factors and require fewer wires and simpler fabrication processes.<sup>17</sup> Despite its potential, limited research has explored the integration of this technology into robotic walkers, presenting a significant opportunity for advancement in this field.

In this sense, the main contribution of this work is the validation of a force sensor based on this novel concept involving optical sensors. Furthermore, how with a data-driven deep learning method it is possible to accurately estimate the applied normal force. Thus, a fully integrated sensor is presented that uses affordable fabrication methods for easy integration into smart walkers, improving functionality, accuracy and reducing complexity and fabrication costs.

## 2. MATERIALS AND METHODS

This section presents the sensor design and fabrication process. Besides, it describes in detail the algorithms implemented in this study to predict the magnitude of the applied force and the location of the contact.

### 2.1 Sensor Design and Manufacturing

The sensor board was designed with 4 individual addressable RGB LEDs (WS2812, World Semiconductor Co, China), 4 resistors of 130  $\Omega$ , 4 capacitors of 0.1  $\mu\text{F}$  and 5 light-sensitive photodiodes (PDs) (OSRAM BPW34S, Vishay Semiconductors, United States). The LEDs were selected for their ability to be controlled independently using a single data line, which simplifies the wiring and reduces the need for additional pins in the control unit. Similarly, the PDs were chosen for their large active sensing area of 7 mm<sup>2</sup>, providing a smooth response as light paths are altered.<sup>17</sup>

Figure 1 presents the sensor. The system was encapsulated in a transparent layer of silicone (Clear Flex 50, Smooth-On, Inc., United States), which serves as a waveguide. This material has a Shore A hardness of 50, offering flexibility while providing moderate resistance to deformation. Additionally, its transparency makes it highly suitable for optical applications. The mixture was prepared in a 1:2 ratio, degassed in a vacuum chamber

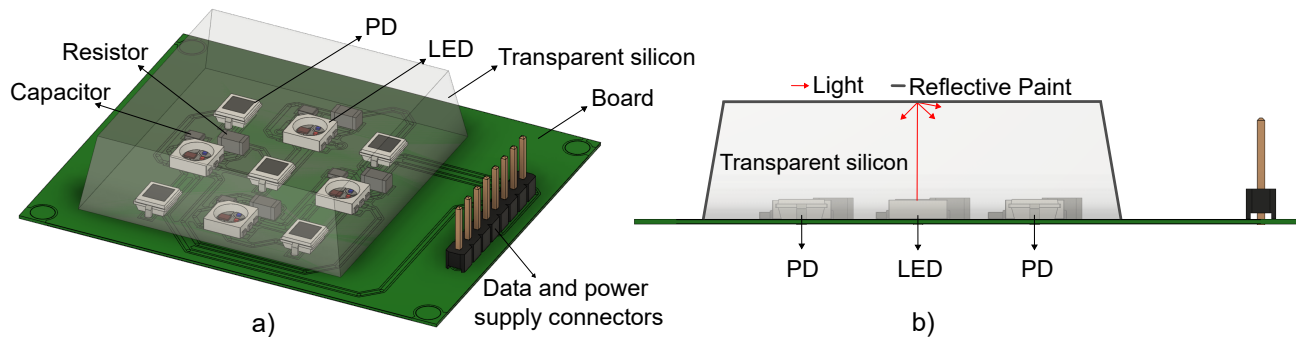


Figure 1. Proposed sensor. a) Sensor architecture from isometric view. b) Sensor configuration viewed from the front. Besides, the basic concept of the sensor is presented where the emitted light is reflected towards the PDs due to the reflective paint.

(Resinagem, Brazil) for 10 minutes, and left to cure at room temperature for 24 hours. To create the flexivel structure with a truncated pyramid shape, a 3d-printed mold made of PLA (Polylactic Acid) was used to house the resin and the PCB (printed circuit board). Finally, to complete the sensor, a thin layer of reflective acrylic paint was applied for two reasons: (1) to reflect light back into the transparent elastomer, preventing outward refraction, and (2) to block ambient light, thus enhancing the sensor's accuracy.

## 2.2 Data collection and Learning Algorithms

For data collection, a load cell (PCE-C-R13LFC, PCE Instruments, Germany) was adapted in a indenter to record force measurements. The process consisted of applying loads ranging from 0 to 55 Newtons. The test was repeated six times to ensure accuracy and consistency of the results (see Figure 2). Additionally, the loads were applied on each PD, which allowed to register the contribution of each one during the tests. This methodological approach made it possible to analyze the interaction and behavior of the sensory components under different loading conditions, which was crucial to understand the dynamics of the system.

On the other hand, the signals produced by the sensor were directly correlated with surface deformation, however, building an analytical model to reconstruct the surface state from the collected data could be a difficult task due to the non-linear interaction between the variables, since the signals change in relation to the deformation of the transparent medium, the relative position of the LEDs and PDs as well as the properties of the material, requiring very precise manufacturing.<sup>17</sup> For this reason, the use of purely data-driven based algorithms was an alternative to estimate the parameters of interest from this set of signals.<sup>17,18</sup> Specifically, this study was focused on determining the location of a contact and the applied normal force.

For the force prediction, a dense neural network configured for regression tasks was implemented, which uses five input features (i.e., the data from the PDs). It was designed with three layers, a first layer of 254 activation units, a second hidden layer of 64 hidden units and a final layer that returns the force value. ReLU (rectified linear unit) was implemented as the activation function and a Dropout technique with a 10% rate to mitigate overfitting. Besides, Adam optimizer was implemented with a learning rate of 0.001, mean square error (MSE) was used as a loss function, and mean absolute error (MAE) was monitored as a performance metric. It was trained with 30 epochs and a batch size of 32, reserving 20% of the data for validation. The activation function, Dropout technique, optimizer, learning rate, loss function, and performance metric were implemented as described in.<sup>17</sup> However, the remaining parameters were experimentally adjusted to achieve the best results.

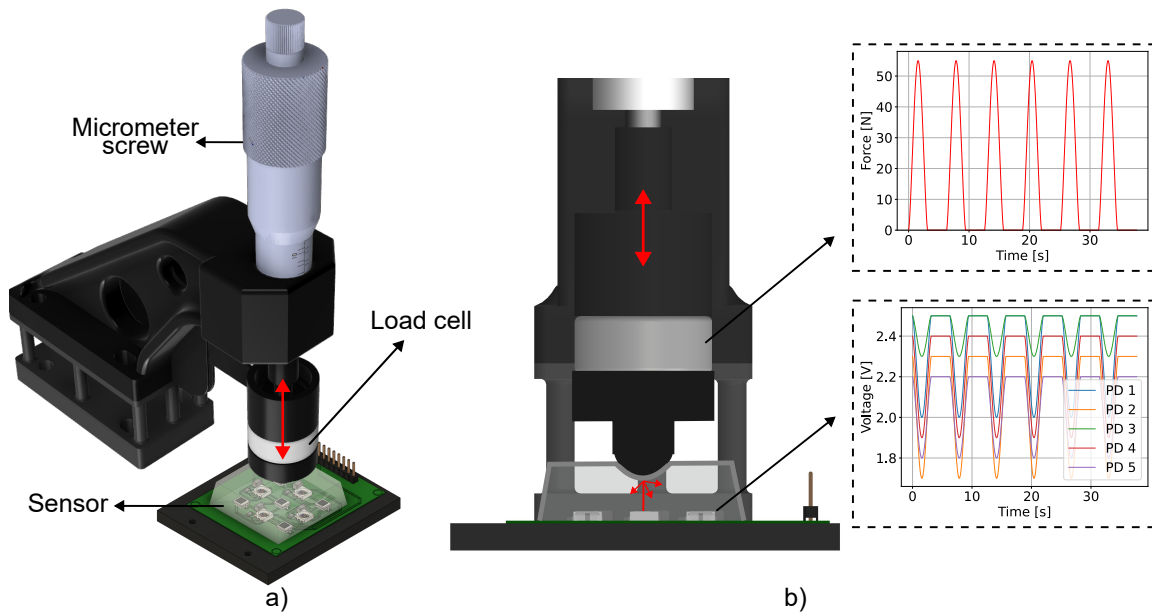


Figure 2. Mechanical set-up for data collection. a) Proposed structure. b) Sensor surface deformation due the contact with the identer.

Regarding the prediction of the zone in which the force was applied, a random forest model was implemented. It was configured with 3 trees and each with a maximum depth of 4 levels. To increase the diversity among the trees in the forest, the parameter was adjusted to randomly select the square root of the total number of features in each node division. This prevents trees becoming too similar and relying on the same dominant features, improving the robustness of the model to variations in the data. Moreover, as regulatory measures, the model was configured for each node to have at least five samples to allow the split and for each leaf to have at least three samples. Finally, the cross-validation technique was used with 40 partitions to provide a robust measure of overall performance while avoiding overfitting.

It is important to highlight that of the six loads that were applied, the data (from both the PDs and the load cell) of the first 5 were used for training and the last one was implemented to evaluate the model's capability to predict the applied force and the zone in which it was applied.

### 3. RESULTS AND DISCUSSION

Figure 3 presents the results obtained when pressure was applied to PD 1. As mentioned previously, 6 repetitions were performed and the contribution of each PD was measured. These results were selected, as the PDs exhibited average performance, compared to all tests.

The PD1, which was directly stimulated, showed a response proportional to the increase of the applied force, evidencing a high sensitivity in the contact region. However, the other PDs also exhibited responses to the force application, although of lesser magnitude. This behavior in the neighboring sensors suggests that the system can detect not only the force applied at a specific point, but also how it is distributed and how the surface is affected. This transverse sensing capability indicates that the sensor has the potential to function as a deformable and fully measurable surface, which could be advantageous in applications where continuously distributed forces need to be monitored, allowing the evaluation of more complex pressure patterns.

On the other hand, Figure 4 presents the response of the models predicting the zone and the applied force based on the data from the PDs. As can be seen, the results demonstrate a high accuracy of the dense neural network, which is evidence of its ability to capture the relationship between the PD data and the applied force. Specifically, an average error of 2.208% was obtained, which remains within the margins reported in.<sup>17</sup> In the case of PD3, the error increased, reaching 2.61%. However, this result is supported by,<sup>17</sup> where increases in the error of up to 5% were reported when working with loads between 9 and 16 N. This increase could be related to the magnitude of the applied load, since the error is mainly observed in the range from 30 to 55 N. However,

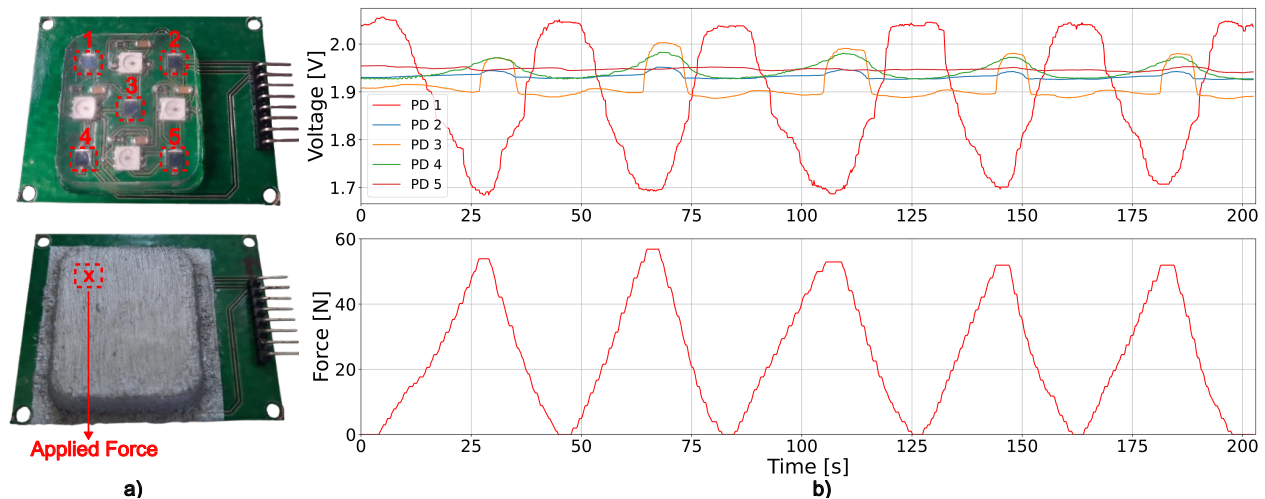


Figure 3. Results obtained from the response of the sensor. a) Sensor configuration, location of the PDs and where the force was performed. b) Contribution of each PD and the force captured from the load cell.

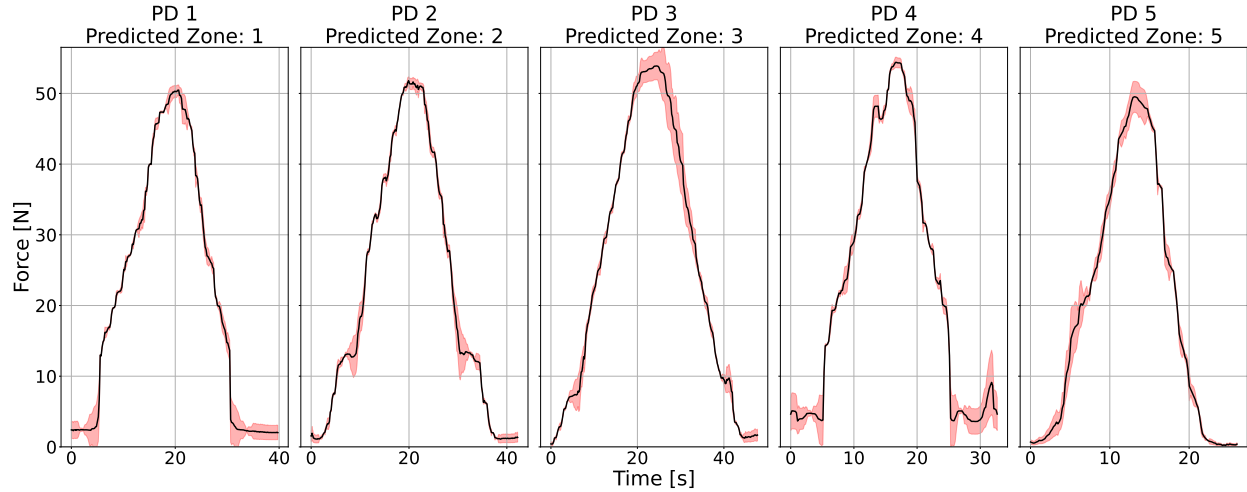


Figure 4. Results obtained from the proposed models. The black line represents the predicted force and the red shadow represents the error with respect to the real data.

when compared to the applied forces in,<sup>17</sup> the error is still relatively low. Moreover, as PD3 is the most central PD, it is more susceptible to the variations, which could induce more complex patterns for the neural network.

As for PD4, it is evidenced a inability to predict forces smaller than 4 N when loads are applied directly on it. As reported in,<sup>17</sup> this result is to be expected, since errors of up to 10% are observed when working with light loads. This suggests that it might be beneficial to reduce the measurement range for low loads in order to maintain the accuracy of the system. According to the literature, forces greater than 5 N have been reported by the user in path-following tasks.<sup>10,19</sup> Additionally, having a sensor with a fully deformable surface, it is possible to implement some technique to compensate this limitation in range of some points.

On the other hand, regarding the classification of the force application zones, the Random Forest model demonstrated outstanding performance. With an accuracy of 0.98 after training, it was able to correctly predict the five zones where loads were applied. This high performance highlights the model's inherent ability to handle complex data and establish clear patterns in multi-categorical classification problems. Furthermore, this result is supported by what is reported in,<sup>18</sup> where the effectiveness of Random Forest in this type of tasks is emphasized, highlighting its robustness to variations in the data and its ability to generalize correctly.

#### 4. CONCLUSIONS AND FUTURE WORK

The design and development of the optical sensor presented in this work offers an innovative and practical solution to overcome the limitations of traditional sensors used in assistive devices. The integration of sensitive PDs and RGB LEDs within a transparent silicon layer allows for highly accurate measurement of applied normal forces, while maintaining a robust, cost-effective and easy-to-fabricate design. This approach significantly reduces complexity and cost, compared to technologies such as strain gauges, piezoelectric sensors, triaxial cells, even other optical technologies like POF or FBGs, extending its viability for smart walker applications.

The results obtained confirm the effectiveness of the proposed system, highlighting the ability of the dense neural network model to predict applied forces with an average error of 2.2% and of the random forest model to classify with 98% accuracy the contact zones. Moreover, it was observed that the sensor can capture both directly applied forces and their distribution on the surface, which opens new possibilities for monitoring more complex pressure patterns in advanced applications. However, slight limitations were identified in the prediction of small forces, suggesting opportunities to adjust the measurement range and optimize performance at lower loads.

Finally, this sensor represents an alternative to physical human-robot interaction strategies. Future work could focus on validating the system (mounted on the handlebar of a robotic walker) in real-world scenarios,

increasing the number of PDs to expand the spatial resolution, and exploring its integration with other advanced sensors. Overall, this breakthrough has the potential to transform the way robotic devices monitor physical interaction with the user to provide more natural and intuitive interactions.

## ACKNOWLEDGMENTS

Camilo A. R. Diaz acknowledges the financial support of FAPES (633/2022, 2022–C5K3H), CNPq (404111/2023–8, 310668/2021–2, 308155/2023–8, 403753/2021–0) and IEEE RAS SPARX. FINEP (Tec assistiva – 2784/20, Tec assistiva 2 – 2132/22)

## REFERENCES

- [1] United Nations, Department of Economic and Social Affairs, “World population ageing 2019,” Tech. Rep. ST/ESA/SER.A/444 (2020).
- [2] World Health Organization, “Ageing and health,” (2018). Accessed: Nov. 2024. [Online]. Available: <https://www.who.int/news-room/fact-sheets/detail/ageing-and-health>.
- [3] Cifuentes, C. A. and Múnera, M., [*Interfacing Humans and Robots for Gait Assistance and Rehabilitation*], vol. 1, Springer International Publishing, 1 ed. (2022).
- [4] Auvinet, B., Touzard, C., Montestruc, F., Delafond, A., and Goeb, V., “Gait disorders in the elderly and dual task gait analysis: a new approach for identifying motor phenotypes,” *Journal of neuroengineering and rehabilitation* **14**, 1–14 (2017).
- [5] Maresova, P., Javanmardi, E., Barakovic, S., Barakovic Husic, J., Tomsone, S., Krejcar, O., and Kuca, K., “Consequences of chronic diseases and other limitations associated with old age—a scoping review,” *BMC public health* **19**, 1–17 (2019).
- [6] Cifuentes, C. A. and Frizera, A., [*Human-robot interaction strategies for walker-assisted locomotion*], vol. 115, Springer (2016).
- [7] Martins, M., Santos, C., Frizera, A., and Ceres, R., “A review of the functionalities of smart walkers,” *Medical engineering & physics* **37**(10), 917–928 (2015).
- [8] Cifuentes, C. A., Múnera, M., Aristizabal-Aristizabal, J., Ferro-Rugeles, R., Lancheros-Vega, M., Sierra M, S. D., Múnera, M., and Cifuentes, C. A., “Fundamentals for the design of smart walkers,” *Interfacing Humans and Robots for Gait Assistance and Rehabilitation* , 121–141 (2022).
- [9] Sierra M, S. D., Garzón, M., Múnera, M., and Cifuentes, C. A., “Human–robot–environment interaction interface for smart walker assisted gait: Agora walker,” *Sensors* **19**(13), 2897 (2019).
- [10] Cifuentes, C. A., Múnera, M., Sierra M, S. D., Jiménez, M. F., Frizera-Neto, A., Múnera, M., and Cifuentes, C. A., “Control strategies for human–robot–environment interaction in assisted gait with smart walkers,” *Interfacing Humans and Robots for Gait Assistance and Rehabilitation* , 259–286 (2022).
- [11] Leal-Junior, A. G., Diaz, C. A., Avellar, L. M., Pontes, M. J., Marques, C., and Frizera, A., “Polymer optical fiber sensors in healthcare applications: A comprehensive review,” *Sensors* **19**(14), 3156 (2019).
- [12] Moreno, J., Bueno, L., Pons, J. L., Baydal-Bertomeu, J., Belda-Lois, J., Prat, J., and Barberá, R., “Wearable robot technologies,” *Wearable robots: biomechatronic exoskeletons*. Hoboken: John Wiley & Sons , 165–99 (2008).
- [13] Leal-Junior, A. G., Díaz, C. R., Marques, C., Pontes, M. J., and Frizera, A., “3d-printed pof insole: Development and applications of a low-cost, highly customizable device for plantar pressure and ground reaction forces monitoring,” *Optics & Laser Technology* **116**, 256–264 (2019).
- [14] Leal-Junior, A. G., Frizera, A., Marques, C., Sanchez, M. R., Botelho, T. R., Segatto, M. V., and Pontes, M. J., “Polymer optical fiber strain gauge for human-robot interaction forces assessment on an active knee orthosis,” *Optical Fiber Technology* **41**, 205–211 (2018).
- [15] Junior, A. L., de Andrade, R. M., and Bento Filho, A., “Series elastic actuator: Design, analysis and comparison,” *Recent Advances in Robotic Systems* **1**(3) (2016).
- [16] Leal-Junior, A., Theodosiou, A., Díaz, C., Marques, C., Pontes, M. J., Kalli, K., and Frizera-Neto, A., “Fiber bragg gratings in cytop fibers embedded in a 3d-printed flexible support for assessment of human–robot interaction forces,” *Materials* **11**(11), 2305 (2018).



- [17] Piacenza, P., Behrman, K., Schifferer, B., Kymissis, I., and Ciocarlie, M., “A sensorized multicurved robot finger with data-driven touch sensing via overlapping light signals,” *IEEE/ASME Transactions on Mechatronics* **25**(5), 2416–2427 (2020).
- [18] Li, T., Zhang, A., Du, M., Zhu, Y., Wang, N., Han, X., Li, X., Tan, Y., and Zhou, Z., “A fingertip optical fiber composite sensor with conformal design for robotic perception of tactile force,” *IEEE/ASME Transactions on Mechatronics* (2024).
- [19] Jimenez, M. F., Mello, R. C., Loterio, F., and Frizera-Neto, A., “Multimodal interaction strategies for walker-assisted gait: A case study for rehabilitation in post-stroke patients,” *Journal of Intelligent & Robotic Systems* **110**(1), 13 (2024).